

**Dynamics of  
~100-kyr glacial  
cycles during the  
early Miocene**

D. Liebrand et al.

# Dynamics of ~100-kyr glacial cycles during the early Miocene

**D. Liebrand<sup>1,\*</sup>, L. J. Lourens<sup>1</sup>, D. A. Hodell<sup>2,\*\*</sup>, B. de Boer<sup>3</sup>, and R. S. W. van de Wal<sup>3</sup>**

<sup>1</sup>Department of Earth Sciences, Faculty of Geosciences, Utrecht University. Budapestlaan 4, 3584 CD Utrecht, The Netherlands

<sup>2</sup>Department of Geological Sciences, University of Florida, 241 Williamson Hall, P.O. Box 112120, Gainesville, Florida 32611, USA

<sup>3</sup>Institute for Marine and Atmospheric research Utrecht (IMAU), Utrecht University, Princetonplein 5, 3584 CC Utrecht, The Netherlands

\* now at: School of Ocean and Earth Science, University of Southampton, National Oceanography Centre, Southampton, European Way, Southampton SO14 3ZH, UK

\*\* now at: Department of Earth Sciences, University of Cambridge, Downing Street, Cambridge CB2 3EQ, UK

Received: 15 November 2010 – Accepted: 7 December 2010 – Published: 20 December 2010

Correspondence to: D. Liebrand (diederik.liebrand@noc.soton.ac.uk)

Published by Copernicus Publications on behalf of the European Geosciences Union.

Title Page

Abstract

Introduction

Conclusions

References

Tables

Figures

⏪

⏩

◀

▶

Back

Close

Full Screen / Esc

Printer-friendly Version

Interactive Discussion



## Abstract

Here, we present high-resolution stable isotope records from ODP Site 1264 in the South-Eastern Atlantic Ocean, which resolve the latest Oligocene to early Miocene (23.7–18.9 Ma) climate changes. Using an inverse modelling technique, we decomposed the oxygen isotope record into temperature and ice volume and found that the Antarctic ice sheet expanded during distinct episodes (e.g., Mi zones) of low short-term (~100-kyr) eccentricity forcing, which occur two to four long-term (400-kyr) eccentricity cycles apart. We argue that a non-linear mechanism, such as the merging of (several) large East Antarctic ice sheets, caused the build-up of a larger ice sheet. During the termination phases of these larger ice sheets, on the contrary, we find a more linear response of ice-sheet variability to orbital forcing and climate became highly sensitive to the ~100-kyr eccentricity cycle. At the Oligocene-Miocene transition the model output indicates a decrease in Northern Hemisphere temperatures such that a small ice cap could develop on Greenland. This Supports the hypothesis of a threshold response for the development of Northern Hemisphere land ice to decreasing  $p\text{CO}_2$ .

## 1 Introduction

Earth's climate has gradually cooled during the past 50 million years in conjunction with declining atmospheric  $p\text{CO}_2$  conditions (Zachos et al., 2008). Following the cooling and rapid expansion of Antarctic continental ice-sheets in the earliest Oligocene, deep-sea oxygen isotope ( $\delta^{18}\text{O}$ ) values remained relatively high (2.5‰), indicating permanent ice cover with a mass as large as 50% of that of the present-day and bottom-water temperatures of  $\sim 4^\circ\text{C}$  (Lear et al., 2004). The Antarctic ice sheets persisted until the later part of the Oligocene (26 to 27 Ma), when a warming trend reduced their volume. This trend persists until the middle Miocene ( $\sim 15$  Ma) with the exception of several brief periods of "glaciation", such as during the Oligocene-Miocene transition (Miller et al., 1991). Initially, two Oligocene and six Miocene oxygen isotope zones

## Dynamics of ~100-kyr glacial cycles during the early Miocene

D. Liebrand et al.

Title Page

Abstract

Introduction

Conclusions

References

Tables

Figures

⏪

⏩

◀

▶

Back

Close

Full Screen / Esc

Printer-friendly Version

Interactive Discussion



(Oi-1, Oi-2, Mi-1-Mi-6) were described (Miller et al., 1991), followed by Mi-1a, Mi-1b, Mi-7, Mi-1aa (Wright and Miller, 1992), Oi-2b.1, Mi-1.1 (Billups et al., 2002) and another, yet unnamed, zone (Paul et al., 2000) for the latest Oligocene and early Miocene.

It has long been suspected that the large-scale changes in Antarctic ice volume are coupled to long-term eccentricity (2.0–2.6 myr) and obliquity (~1.2 myr) modulations of the Earth's orbit and axial tilt (Miller et al., 1991; Wright and Miller, 1992; Beaufort, 1994; Lourens and Hilgen, 1997). This theory could only recently be investigated with the generation of high-resolution ( $\leq 10$  kyr) oxygen isotope records (Zachos et al., 2001b; Pälike et al., 2006a, b; Billups et al., 2002). Here we will assess the long-term orbital pacing theory of the late Oligocene to early Miocene (~19–24 Ma) time interval by presenting a new high-resolution (<3 kyr) and continuous stable isotope record based on the benthic foraminiferal species *Cibicoides mundulus* from Ocean Drilling Program (ODP) Site 1264 situated at a water depth of 2505 m on the northern flank of the Walvis Ridge (29° S) in the Southern Atlantic Ocean (Zachos et al., 2004). We will compare our isotope results with those of ODP Site 926 Hole B (3° N) at 3598 m water depth and ODP Site 929 Hole A (6° N) at 4358 m water depth, both from Ceara Rise in the Equatorial Western Atlantic (Zachos et al., 1997, 2001b; Paul et al., 2000; Pälike et al., 2006a; Shackleton et al., 2000), and the composite record of ODP Site 1090, based on Holes D and E, at 3699 m water depth from the Agulhas Ridge (43° S) in the Atlantic section of the Southern Ocean (Billups et al., 2002, 2004). In addition, through an inverse modelling technique we have decomposed the marine benthic  $\delta^{18}\text{O}$  record into temperature and Northern Hemisphere and Antarctic ice volume contributions (De Boer et al., 2010; Bintanja and Van de Wal, 2008).

## Dynamics of ~100-kyr glacial cycles during the early Miocene

D. Liebrand et al.

Title Page

Abstract

Introduction

Conclusions

References

Tables

Figures

⏪

⏩

◀

▶

Back

Close

Full Screen / Esc

Printer-friendly Version

Interactive Discussion

## 2 Site descriptions and age model

### 2.1 Site 1264 and Site 1265

In 2003, the Ocean Drilling Program (ODP) revisited Walvis Ridge in the South-Eastern Atlantic Ocean during Leg 208 (Zachos et al., 2004). Six sites were drilled along a depth-transect of which two sites, Site 1264 (2505 m) and 1265 (3083 m), are used in this study. Both sites are – and were throughout the entire Neogene – situated above the level of the present day lysocline and CCD (Zachos et al., 2004). The extended late Oligocene and early Miocene section of Site 1264 consists of foraminifer bearing nannofossil ooze (Zachos et al., 2004). Site 1264 is uniquely situated (Fig. 1) to record major changes in regional and/or global ocean carbon chemistry, ocean circulation and intermediate bottom water chemistry and circulation (Zachos et al., 2004). Site 1265 was applied to provide the magnetic inclination record that Site 1264 lacks.

### 2.2 Age model

Because Site 1264 lacks a good magnetostratigraphy, we transferred the magnetostratigraphic data from the nearby ODP Site 1265 by pattern matching the magnetic susceptibility (MS) and colour reflectance (CR, 600/450 nm) records (Fig. 2, Table 1). Subsequently we assigned the ATNTS2004 ages (Lourens et al., 2004) (Astronomically Tuned Neogene Time Scale) to the magnetic reversals and applied a third order polynomial to inter- and extrapolate the age model. This resulted in an orbital-based age model without tuning individual peaks to the astronomical solution. We chose to present our data on an un-tuned, but loosely astronomy based, timescale to re-examine previous interpretations about the Oligocene and Miocene climate dynamics. Finally, the “Match” algorithm (Lisiecki and Lisiecki, 2002) was applied to correlate the stable isotope records of Ceara Rise and the Agulhas Ridge to Site 1264 (Fig. 3).

CPD

6, 2741–2766, 2010

## Dynamics of ~100-kyr glacial cycles during the early Miocene

D. Liebrand et al.

Title Page

Abstract

Introduction

Conclusions

References

Tables

Figures

⏪

⏩

◀

▶

Back

Close

Full Screen / Esc

Printer-friendly Version

Interactive Discussion



### 3 Stable isotopes

#### 3.1 Methodology and stable isotope chemistry

Samples of approximately 10 g of sediment were taken every 2–2.5 cm from the latest Oligocene and early Miocene part of the Site 1264. The samples were freeze dried, washed and sieved to obtain the larger than 37, 65 and 125  $\mu\text{m}$  fractions for foraminiferal analysis. Mostly single specimen samples of the benthic foraminifer species *Cibicidoides mundulus* were analysed. On every sample stable oxygen and carbon isotope ratios ( $\delta^{18}\text{O}$  and  $\delta^{13}\text{C}$ , respectively) were measured and the  $\delta^{18}\text{O}$  values were corrected for disequilibrium with seawater by adding 0.64‰ (Shackleton, 1974; Zachos et al., 2001a). Approximately 80% of the samples were measured at the Faculty of Geosciences of Utrecht University (UU) where foraminiferal tests were dissolved in a Finnigan MAT Kiel III automated preparation system. Isotopic ratios of purified  $\text{CO}_2$  gas were then measured on-line with a Finnigan MAT 253 mass spectrometer and compared to an internal gas standard. The remaining part was measured at the Department of Geological Sciences of the University of Florida (UF) on two inter-calibrated devices. Of the samples with plentiful specimens, foraminiferal calcite was reacted using a common acid bath of orthophosphoric acid at 90 °C using a Micro-mass Isocarb preparation system. Isotope ratios of purified  $\text{CO}_2$  gas were measured online using a Micromass Prism mass spectrometer. Of the samples with few *Cibicidoides mundulus* specimens, foraminiferal tests were dissolved using a Finnigan MAT Kiel III automated preparation system coupled to a Finnigan MAT 252 mass spectrometer to measure the isotopic ratios of purified  $\text{CO}_2$  gas. The standard NBS-19 and the in-house (at UU) standard “Naxos” were used to calibrate to Vienna Pee Dee Belemnite (VPDB). Reproducibility (same sample on the same device) is 0.19‰ for  $\delta^{18}\text{O}$  and 0.13‰ for  $\delta^{13}\text{C}$  (Supplement Fig. 1). Between universities an unexplained offset of 0.30‰ in  $\delta^{18}\text{O}$  is found between analyses of foraminifera from the same samples (Supplement Fig. 1), perhaps due to intraspecific variability (i.e. different (mostly) single specimens from the same sample were analysed) in the duplicate dataset. No

## Dynamics of ~100-kyr glacial cycles during the early Miocene

D. Liebrand et al.

Title Page

Abstract

Introduction

Conclusions

References

Tables

Figures

◀

▶

◀

▶

Back

Close

Full Screen / Esc

Printer-friendly Version

Interactive Discussion



correction has been applied for this offset because a lower resolution (step size 100-kyr) record, spanning the interval of this study, measured entirely at UF shows no offset (B. D. A. Naafs, personal communication, 2010). Outliers were defined by an upper and lower boundary of 2 standard deviations (of the entire time series) added or subtracted from a 13-point moving average. Because the stable isotope analysis is paired, outliers defined in  $\delta^{13}\text{C}$  or in  $\delta^{18}\text{O}$  were removed from both records (Fig. 4, Supplement Fig. 2). Where possible, outliers were re-measured. After outlier-removal the stable isotope records of Site 1264 contain 1754 data points.

### 3.2 Stable isotope stratigraphy

The  $\delta^{18}\text{O}$  record of Site 1264 overlies that of the Agulhas Ridge Site 1090 very well (Fig. 3). Both records are, however,  $\sim 0.5\%$  heavier than the  $\delta^{18}\text{O}$  records of Sites 926 and 929. This offset may point to a difference in the oxygen isotopic composition of the water masses and/or calcification temperature between the sites. In particular, North Atlantic (Billups et al., 2002) or a Tethyan-Pacific (Von der Heydt and Dijkstra, 2006) through-flow may have brought in warmer water masses at the depth of the Ceara Rise sites during this time period. The  $\sim 0.4\%$  difference in the average  $\delta^{18}\text{O}$  values before and after Mi-1 at Ceara Rise (Zachos et al., 2001b) is not recorded at Site 1264, suggesting that a possible Oligocene to Miocene flow reversal through the Panamanian Seaway (Von der Heydt and Dijkstra, 2006) or changes in abyssal circulation patterns in the Atlantic (Miller and Fairbanks, 1983) did not significantly alter the  $\delta^{18}\text{O}$  composition of the Southern Atlantic deep waters. The carbon isotope record of Site 1264 is on average 0.1 to 0.4% heavier than those of Sites 1090, 926 and 929 (Fig. 3). The highest  $\delta^{13}\text{C}$  value of almost 2.0% coincides with the onset of the Oligocene-Miocene Carbon Maximum, CM-OM (Hodell and Woodruff, 1994), and concur (Zachos et al., 1997) with the maximum  $\delta^{18}\text{O}$  values during Mi-1. The sudden decline in  $\delta^{13}\text{C}$  values of  $\sim 0.4\%$  that marks the end of the CM-OM around  $\sim 21.8$  Ma coincides with a significant change in the deep-sea carbon reservoir within the entire Atlantic Ocean (Figs. 3, 4).

## Dynamics of $\sim 100$ -kyr glacial cycles during the early Miocene

D. Liebrand et al.

Title Page

Abstract

Introduction

Conclusions

References

Tables

Figures

⏪

⏩

◀

▶

Back

Close

Full Screen / Esc

Printer-friendly Version

Interactive Discussion





**Dynamics of  
~100-kyr glacial  
cycles during the  
early Miocene**

D. Liebrand et al.

Title Page

Abstract

Introduction

Conclusions

References

Tables

Figures

⏪

⏩

◀

▶

Back

Close

Full Screen / Esc

Printer-friendly Version

Interactive Discussion



is equivalent to the amount of land-ice storage in Antarctica and on the Northern Hemisphere (mainly Greenland). On average,  $\delta_w$  leads  $\delta_T$  by  $\sim 7$  kyr, implying that ice-sheet growth precedes polar cooling, in contrast to previous findings (Bintanja and Van de Wal, 2008). The outcome of our ice-sheet model simulations show that changes in  $\delta^{18}\text{O}$  are accompanied by large shifts in  $\Delta T_{\text{NH}}$  (Fig. 6, Supplement Fig. 3). Minimum NH air temperatures of  $\sim 4^\circ\text{C}$  were reached during Mi-1 ( $\sim 23.1$  Ma) and caused a small ice sheet to develop on Greenland, which may have contributed to a global sea level lowering in the order of 20 to 30 cm (Fig. 6). These findings are in agreement with the expected  $p\text{CO}_2$  threshold described for NH land-ice at  $\sim 280$  ppmv (DeConto et al., 2008) and the reconstructed drop in atmospheric  $\text{CO}_2$  levels approaching that value within error (Kürschner et al., 2008; Pagani et al., 1999). An extra sensitivity experiment has been applied to test the significance of the Northern Hemisphere contribution to sea level lowering across the Oligocene-Miocene boundary. Present day  $\delta^{18}\text{O}$  values (pdv) were varied from 3‰ to 3.5‰ with 0.05‰ increments. This resulted in a 7 m sea level lowering at 3‰ pdv and no NH ice cap at 3.5‰ pdv. The former situation would equal present day NH ice volume, while the latter scenario would mean no NH ice was present during this enduring period of global cooling. We regard both options as unrealistic for this time and perceive 3.23‰ pdv as most probable. The main sea level changes are associated, however, with ice sheet fluctuations on Antarctica of up to  $\sim 40$  meter sea level equivalent (m.s.l.e.) around 23 million years ago. At this time, the combined West and East Antarctic ice sheet reached their maximum size and volume of the time interval studied, resulting in a global sea level of  $\sim 2.5$  m above present-day, indicating that the Antarctic ice sheet attained (almost) its present-day size.

Wavelet analyses of the separate sea level and temperature components of  $\delta^{18}\text{O}$  revealed an almost similar pattern as the  $\delta^{18}\text{O}$  record. The episodes of  $\sim 100$ -kyr dominated  $\delta^{18}\text{O}$  variability, and resultant  $\sim 100$ -kyr dominated ice volume and  $\Delta T_{\text{NH}}$ , are preceded by an interval of gradual cooling and glacial build-up. In fact, the  $\sim 100$ -kyr dominated episodes seem to coincide with the termination phase of periods (e.g., Mi-events) of large Antarctic ice sheet expansion (Figs. 4, 6).

## 5 Multiple early Miocene ~100-kyr worlds

Following the astronomical naming scheme based on the 400-kyr cycle of Earth's eccentricity (Wade and Pälike, 2004), Mi-1 starts within cycle 58 at ~23.4 Ma and it ends within cycle 57 at ~22.6 Ma (Figs. 4, 6). Similar patterns are reflected by the ice-sheet build-up phases at 22.3–21.9 Ma (cycles 56–55), 21.6–21.1 Ma (cycles 54–53), and 20.2–19.4 Ma (cycles 50–49) of which the latter two periods are close within the age estimates of the Mi-1a and Mi-1aa episodes (Wright and Miller, 1992), respectively (Fig. 7).

The build-up phases (large-scale Antarctic ice-sheet expansions) seem to occur as a result of a weak imprint of the ~100-kyr eccentricity-related climate cycles. According to our age model, these intervals are not perfectly aligned to either a node in the ~2.4 myr modulation of eccentricity nor to a node in the ~1.2 myr modulation of obliquity (Fig. 4). They do appear, however, during short intervals in which the power of the ~100-kyr eccentricity cycle is significantly suppressed (e.g. the 400-kyr minima at ~23.1, ~22.3, ~21.4, and ~19.8 Ma, black arrows in Fig. 4). Since the timing of these ice-sheet build-up phases occur two and four 400-kyr eccentricity cycles apart, this suggest that a long-term non-linear mechanism of some kind may have modulated the dominantly eccentricity-paced Antarctic ice-sheet expansions and retreat during the late Oligocene and early Miocene. An example of a non-linear mechanism could be the merging of (several) large East Antarctic ice-sheets (DeConto and Pollard, 2003), which may have resulted in an ice cap of significant proportions that survived the relatively warm global climate conditions during a weak eccentricity maximum; analogous to the mechanism proposed for the Mid Pleistocene Transition where the Laurentide and Corderillan ice sheets merged (Bintanja and Van de Wal, 2008). It is still possible that this non-linear mechanism derived from a pre-conditioning of the Antarctic ice sheets by changes in the Earth's obliquity, since this cycle strongly determines insolation variations at high latitudes. Although the imprint of obliquity on the  $\delta^{18}\text{O}$  record of Site 1264 is weaker, its clear presence in the Ceara Rise records indicates that

CPD

6, 2741–2766, 2010

### Dynamics of ~100-kyr glacial cycles during the early Miocene

D. Liebrand et al.

Title Page

Abstract

Introduction

Conclusions

References

Tables

Figures

⏪

⏩

◀

▶

Back

Close

Full Screen / Esc

Printer-friendly Version

Interactive Discussion

the Antarctic ice fluctuations are at least partly controlled by high-latitude insolation changes (Zachos et al., 1997, 2001b; Paul et al., 2000; Pälike et al., 2006a). Given our age constraints, the link between the long-term ( $\sim 1.2$  myr) obliquity modulation and the ice-sheet build-up phases are as yet too inconsistent to suggest any causal relationship between them (Fig. 4). Our findings thus imply a greater non-linearity in the early Miocene climate system to internal ice-sheet dynamics, which may have caused the (Mi-) episodes of large Antarctic ice-sheet expansion. These episodes were then followed by enhanced climate variability on  $\sim 100$ -kyr timescales during their termination phases. Thus, although the long-term (two or four 400-kyr cycles) pacing of ice-sheet build-up phases is probably controlled by (a) non-linear mechanism(s), their accompanying termination phases are, for a relatively briefer period of time ( $\leq 400$ -kyr), characterised by a greater linear climatic response to (weak or strong)  $\sim 100$ -kyr eccentricity cyclicity (Lisiecki, 2010). The more symmetrical terminations of the individual  $\sim 100$ -kyr cycles during the Oligocene-Miocene transition clearly illustrate this enhanced linearity of the Antarctic ice-sheet (Fig. 4). The consecutive ice-sheet build-up phases followed by enhanced climate variability in response to the  $\sim 100$ -kyr eccentricity cycle were most probably the major causes of environmental change and species turnover (Van Dam et al., 2006) during the early Miocene.

**Supplementary material related to this article is available online at:**

**<http://www.clim-past-discuss.net/6/2741/2010/cpd-6-2741-2010-supplement.pdf>.**

*Acknowledgements.* We are indebted to Geert Ittman, Arnold van Dijk, Jan Drenth, Jason Curtis, Giana Brown, Walter Hale, Gert-Jan Reichart, Christian Zeeden and Klaudia Kuiper for their (technical) assistance. Heiko Pälike, David Naafs, Martin Ziegler, Clara Bolton, Steven Bohaty, Lucy Stap, Tanja Kouwenhoven, Sietske Batenburg, Frits Hilgen, Ellen Thomas, Dick Kroon, Paul Wilson, Eelco Rohling and editor(s)/reviewers are thanked for sharing their ideas on how to improve the science and/or commenting on an earlier version of this manuscript. This

## Dynamics of $\sim 100$ -kyr glacial cycles during the early Miocene

D. Liebrand et al.

Title Page

Abstract

Introduction

Conclusions

References

Tables

Figures



Back

Close

Full Screen / Esc

Printer-friendly Version

Interactive Discussion



research used samples provided by the Ocean Drilling Program and has been made possible by a NWO VIDJ-grant n° [864.02.007] assigned to L. J. L. and European Community's Seventh Framework Programme (FP7/2007-2013) under grant agreement n° [215458] to the GTS-next project.

## 5 References

- Beaufort, L.: Climatic importance of the modulation of the 100 kyr cycle inferred from 16 myr long miocene records, *Paleoceanography*, 9, 821–834, 1994.
- Berggren, W. A., Kent, D. V., Swisher, C. C., and Aubry, M.-P.: A Revised Cenozoic Geochronology and Chronostratigraphy, 54, 129–212, 1995.
- 10 Billups, K., Channell, J. E. T., and Zachos, J.: Late Oligocene to early Miocene geochronology and paleoceanography from the subantarctic South Atlantic, *Paleoceanography*, 17, doi:10.1029/2000PA000568, 2002.
- Billups, K., Pälike, H., Channell, J. E. T., Zachos, J., and Shackleton, N. J.: Astronomic calibration of the late Oligocene through early Miocene geomagnetic polarity time scale, *Earth Planet. Sc. Lett.*, 224, 33–44, 2004.
- 15 Bintanja, R. and Van de Wal, R. S. W.: North American ice-sheet dynamics and the onset of 100 000-year glacial cycles, *Nature*, 454, 869–872, 2008.
- Bintanja, R., Van de Wal, R. S. W., and Oerlemans, J.: Modelled atmospheric temperatures and global sea levels over the past million years, *Nature*, 437, 125–128, 2005.
- 20 Bowles, J.: Data report: revised magnetostratigraphy and magnetic mineralogy of sediments from Walvis Ridge, Leg 208, in: Proc. ODP, Sci. Results, 208: College Station, TX (Ocean Drilling Program), edited by: Kroon, D., Zachos, J. C., and Richter, C., 1-24, doi:10.2973/odp.proc.sr.208.206.2006, 2006.
- De Boer, B., Van de Wal, R. S. W., Bintanja, R., Lourens, L. J., and Tuentler, E.: Cenozoic global ice-volume and temperature simulations with 1-D ice-sheet models forced by benthic  $\delta^{18}\text{O}$  records, *Ann. Glaciol.*, 51, 23–33, 2010.
- DeConto, R. M. and Pollard, D.: A coupled climate-ice sheet modeling approach to the early Cenozoic history of the Antarctic ice sheet, *Palaeogeogr. Palaeoclimatol.*, 198, 39–52, 2003.
- DeConto, R. M., Pollard, D., Wilson, P. A., Pälike, H., Lear, C. H., and Pagani, M.: Thresholds for Cenozoic bipolar glaciation, *Nature*, 455, 652–656, 2008.
- 30

## Dynamics of ~100-kyr glacial cycles during the early Miocene

D. Liebrand et al.

Title Page

Abstract

Introduction

Conclusions

References

Tables

Figures



Back

Close

Full Screen / Esc

Printer-friendly Version

Interactive Discussion



**Dynamics of  
~100-kyr glacial  
cycles during the  
early Miocene**

D. Liebrand et al.

[Title Page](#)[Abstract](#)[Introduction](#)[Conclusions](#)[References](#)[Tables](#)[Figures](#)[⏪](#)[⏩](#)[◀](#)[▶](#)[Back](#)[Close](#)[Full Screen / Esc](#)[Printer-friendly Version](#)[Interactive Discussion](#)

- Grinsted, A., Moore, J. C., and Jevrejeva, S.: Application of the cross wavelet transform and wavelet coherence to geophysical time series, *Nonlinear Proc. Geoph.*, 11, 561–566, 2004.
- Hodell, D. A. and Woodruff, F.: Variations in the strontium isotopic ratio of seawater during the Miocene: stratigraphic and geochemical implications, *Paleoceanography*, 9, 405–426, 1994.
- 5 Kürschner, W. M., Kvacek, Z., and Dilcher, D. L.: The impact of Miocene atmospheric carbon dioxide fluctuations on climate and the evolution of terrestrial ecosystems, *P. Natl. Acad. Sci. USA*, 105, 449–453, 2008.
- Laskar, J., Robutel, P., Joutel, F., Gastineau, M., Correia, A. C. M., and Levrard, B.: A long-term numerical solution for the insolation quantities of the Earth, *Astron. Astrophys.*, 428, 261–285, 2004.
- 10 Lear, C. H., Rosenthal, Y., Coxall, H. K., and Wilson, P. A.: Late Eocene to early Miocene ice sheet dynamics and the global carbon cycle, *Paleoceanography*, 19, PA4015, doi:10.1029/2004PA001039, 2004.
- Lisiecki, L. E.: Links between eccentricity forcing and the 100 000-year glacial cycle, *Nat. Geosci.*, 3, 349–352, 2010.
- 15 Lisiecki, L. E. and Lisiecki, P. A.: Application of dynamic programming to the correlation of paleoclimate records, *Paleoceanography*, 17(4), 1049, doi:10.1029/2001PA000733, 2002.
- Lourens, L. J. and Hilgen, F. J.: Long-periodic variations in the Earth's obliquity and their relation to third-order eustatic cycles and late Neogene glaciations, *Quatern. Int.*, 40, 43–52, 1997.
- 20 Lourens, L., Hilgen, F., Shackleton, N. J., Laskar, J., and Wilson, D.: The Neogene period, in: *A Geologic Time Scale 2004*, edited by: Gradstein, F., Ogg, J., and Smith, A., Cambridge University Press, Cambridge, New York, Melbourne, 2004.
- Miller, K. G. and Fairbanks, R. G.: Evidence for Oligocene-middle Miocene abyssal circulation changes in the Western North Atlantic, *Nature*, 306, 250–253, 1983.
- 25 Miller, K. G., Wright, J. D., and Fairbanks, R. G.: Unlocking the ice house: Oligocene-Miocene oxygen isotopes, eustasy and margin erosion, *J. Geophys. Res.*, 96, 6829–6848, 1991.
- Oslick, J. S., Miller, K. G., Feigenson, M. D., and Wright, J. D.: Oligocene-Miocene strontium isotopes: stratigraphy revisions and correlations to an inferred glacioeustatic record, *Paleoceanography*, 9, 427–443, 1994.
- 30 Pagani, M., Arthur, M. A., and Freeman, K. H.: Miocene evolution of atmospheric carbon dioxide, *Paleoceanography*, 14, 273–292, 1999.
- Paillard, D., Labeyrie, L., and Yiou, P.: Macintosh program performs time-series analysis, *Eos Trans. AGU*, 77, 379, 1996.

## Dynamics of ~100-kyr glacial cycles during the early Miocene

D. Liebrand et al.

[Title Page](#)
[Abstract](#)
[Introduction](#)
[Conclusions](#)
[References](#)
[Tables](#)
[Figures](#)




[Back](#)
[Close](#)
[Full Screen / Esc](#)
[Printer-friendly Version](#)
[Interactive Discussion](#)


- Pälike, H., Frazier, J., and Zachos, J. C.: Extended orbitally forced palaeoclimatic records from the Equatorial Atlantic Ceara Rise, *Quaternary Sci. Rev.*, 25, 3138–3149, 2006a.
- Pälike, H., Norris, R. D., Herrle, J. O., Wilson, P. A., Coxall, H. K., Lear, C. H., Shackleton, N. J., Tripathi, A. K., and Wade, B. S.: The heartbeat of the Oligocene climate system, *Science*, 314, 1894–1898, 2006b.
- Paul, H. A., Zachos, J. C., Flower, B. P., and Tripathi, A.: Orbitally induced climate and geochemical variability across the Oligocene/Miocene boundary, *Paleoceanography*, 15, 471–485, 2000.
- Schlitzer, R.: Ocean data view 4, version 4.3.6, available at: <http://odv.awi.de>, last access: November 2010, 2010.
- Shackleton, N. J.: Attainment of isotope equilibrium between ocean water and the benthonic foraminifera genus *uivergerina*: isotopic changes in the ocean during the last glacial, *Colloq. Int. Ctr. National Rech. Sci.*, 219, 203–209, 1974.
- Shackleton, N. J., Hall, M. A., Raffi, I., Tauxe, L., and Zachos, J. C.: Astronomical calibration age for the Oligocene-Miocene boundary, *Geology*, 28, 447–450, doi:10.1130/0091-7613(2000)28<447:acafto>2.0.co, 2, 2000.
- Torrence, C. and Compo, G. P.: A practical guide to wavelet analysis, *B. Am. Meteorol. Soc.*, 79, 61–78, 1998.
- Van Dam, J. A., Abdul Aziz, H., Angeles Alvarez Sierra, M., Hilgen, F. J., van den Hoek Ostende, L. W., Lourens, L. J., Mein, P., van der Meulen, A. J., and Pelaez-Campomanes, P.: Long-period astronomical forcing of mammal turnover, *Nature*, 443, 687–691, 2006.
- Von der Heydt, A. and Dijkstra, H. A.: Effect of ocean gateways on the global ocean circulation in the late Oligocene and early Miocene, *Paleoceanography*, 21, PA1011, doi:10.1029/2005PA001149, 2006.
- Wade, B. S. and Pälike, H.: Oligocene climate dynamics, *Paleoceanography*, 19, PA4019, doi:10.1029/2004PA001042, 2004.
- Wright, J. D. and Miller, K. G.: Miocene stable isotope stratigraphy, site 747, Kerguelen plateau, *Proceedings of the Ocean Drilling Program, Scientific Results, Scientific Results, Vol. 120*, in Wise, S. W., Jr., Schlich, R., et al., *Proc. ODP, Sci. Results, 120: College Station, TX (Ocean Drilling Program)*, 855–866, 1992.
- Wright, J. D., Miller, K. G., and Fairbanks, R. G.: Early and middle Miocene stable isotopes: implications for deepwater circulation and climate, *Paleoceanography*, 7, 357–389, 1992.
- Zachos, J. C., Flower, B. P., and Paul, H. A.: Orbitally paced climate oscillations across the

**Dynamics of  
~100-kyr glacial  
cycles during the  
early Miocene**

D. Liebrand et al.

[Title Page](#)[Abstract](#)[Introduction](#)[Conclusions](#)[References](#)[Tables](#)[Figures](#)[Back](#)[Close](#)[Full Screen / Esc](#)[Printer-friendly Version](#)[Interactive Discussion](#)

Oligocene/Miocene boundary, *Nature*, 388, 567–570, 1997.

Zachos, J. C., Pagani, M., Sloan, L., Thomas, E., and Billups, K.: Trends, rhythms, and aberrations in global climate 65 ma to present, *Science*, 292, 686–693, 2001a.

Zachos, J. C., Shackleton, N. J., Revenaugh, J. S., Palike, H., and Flower, B. P.: Climate response to orbital forcing across the Oligocene-Miocene boundary, *Science*, 292, 274–278, 2001b.

Zachos, J. C., Kroon, D., Blum, P., Shipboard Scientific Party: Proc. ODP, Init. Repts., 208: College Station, TX (Ocean Drilling Program), doi:10.2973/odp.proc.ir.208.2004, 2004.

Zachos, J. C., Dickens, G. R., and Zeebe, R. E.: An early cenozoic perspective on greenhouse warming and carbon-cycle dynamics, *Nature*, 451, 279–283, 2008.

## Dynamics of ~100-kyr glacial cycles during the early Miocene

D. Liebrand et al.

[Title Page](#)
[Abstract](#)
[Introduction](#)
[Conclusions](#)
[References](#)
[Tables](#)
[Figures](#)
[⏪](#)
[⏩](#)
[◀](#)
[▶](#)
[Back](#)
[Close](#)
[Full Screen / Esc](#)
[Printer-friendly Version](#)
[Interactive Discussion](#)
**Table 1.** Chron ages.

Chron	Site 1265 Mid-point Depth (mcd) <sup>a</sup>	Site 1264 Mid-point Depth (mcd) <sup>b</sup>	ATNTS- 2004 Age (Ma) <sup>c</sup>	3rd order polynomial age (Ma) <sup>d</sup>
C5En (o)	89.745	214.408	18.524	18.564
C6n (y)	90.395	214.878	18.748	18.644
C6n (o)	97.095	221.450	19.722	19.592
C6An (y)	100.420	225.520	20.040	20.102
C6An (o)	105.595	231.792	20.709	20.826
C6Bn (y)	112.720	239.685	21.767	21.662
C6Bn (o)	118.595	245.615	22.268	22.261
C6Cn.1n (y)	121.500	248.937	22.564	22.593
C6Cn.1n (o)	122.390	250.333	22.754	22.733
C6Cn.2n (y)	124.110	252.323	22.902	22.934
C6Cn.2n (o)	124.815	253.342	23.030	23.037
C6Cn.3n (y)	126.145	255.298	23.230	23.237
C6Cn.3n (o)	126.740	256.070	23.340	23.317

<sup>a</sup> Midpoints between the top and bottom uncertainties in magnetic reversals (Bowles, 2006). Depth scale is in meters composite depth (mcd).

<sup>b</sup> Based on calibration shown in Fig. 2.

<sup>c</sup> Astronomically Tuned Neogene Time Scale (Lourens et al., 2004).

<sup>d</sup> 3rd order polynomial based on the ATNTS2004 (Lourens et al., 2004) graphed in Fig. 2.

## Dynamics of ~100-kyr glacial cycles during the early Miocene

D. Liebrand et al.

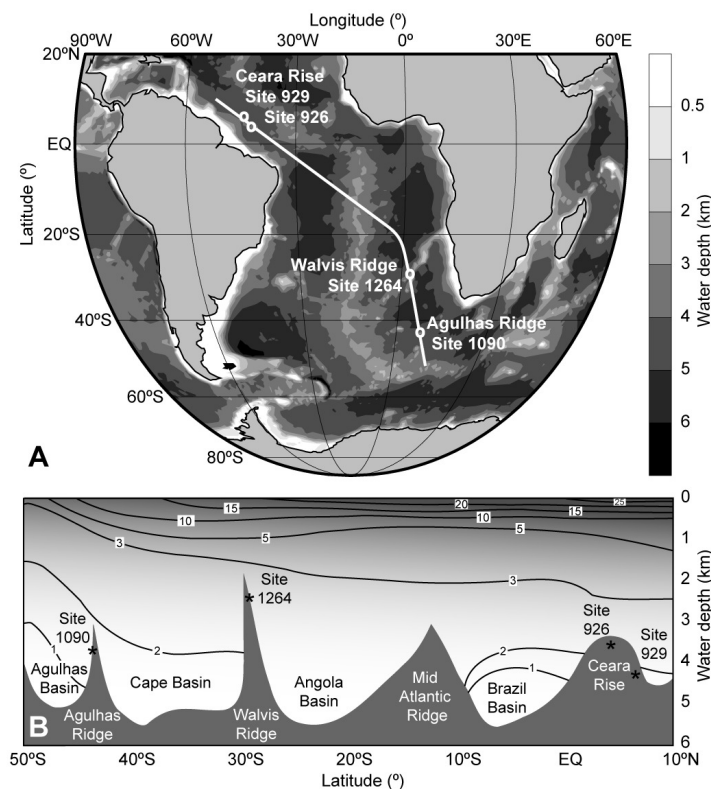


**Fig. 1.** Site locations and Atlantic Ocean transect. **(A)** Present day map of the drill locations of ODP Sites 929, 926, 1264 and 1090. The white line through the drill locations represents the approximate track of the transect shown in **(B)**. **(B)** Transect through the current Equatorial and Southern Atlantic Ocean. Black stars represent drill locations. Black lines represent present day water temperatures. Both graphs were constructed using Ocean Data View (Schlitzer, 2010) and were then graphically edited.

[Title Page](#)
[Abstract](#)
[Introduction](#)
[Conclusions](#)
[References](#)
[Tables](#)
[Figures](#)
[⏪](#)
[⏩](#)
[⏴](#)
[⏵](#)
[Back](#)
[Close](#)
[Full Screen / Esc](#)
[Printer-friendly Version](#)
[Interactive Discussion](#)

## Dynamics of ~100-kyr glacial cycles during the early Miocene

D. Liebrand et al.

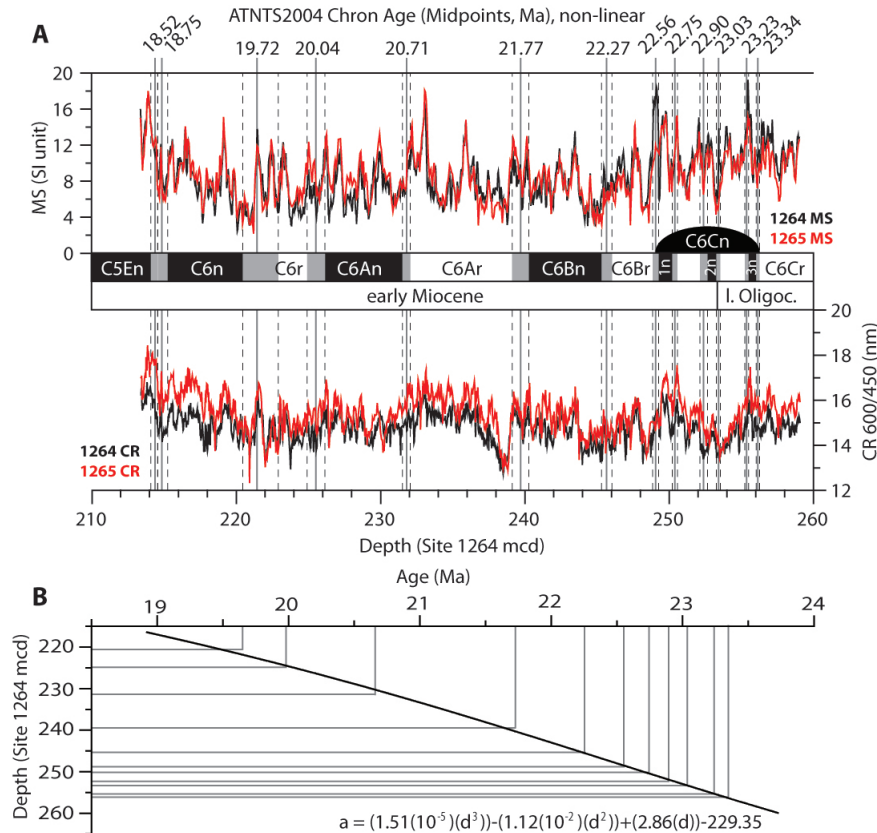


**Fig. 2.** The age model. **(A)** Transfer of the magnetostratigraphy (Bowles, 2006) from Site 1265 to Site 1264 by means of magnetic susceptibility (MS) and 600/450 nm colour reflectance (CR) pattern matching. Depth scale is in meters composite depth (mcd). **(B)** 3rd order polynomial fit through ATNTS2004 (Astronomically Tuned Neogene Time Scale, Lourens et al., 2004) chron ages.

# Dynamics of ~100-kyr glacial cycles during the early Miocene

D. Liebrand et al.

Title Page

Abstract

Introduction

Conclusions

References

Tables

Figures

⏪

⏩

◀

▶

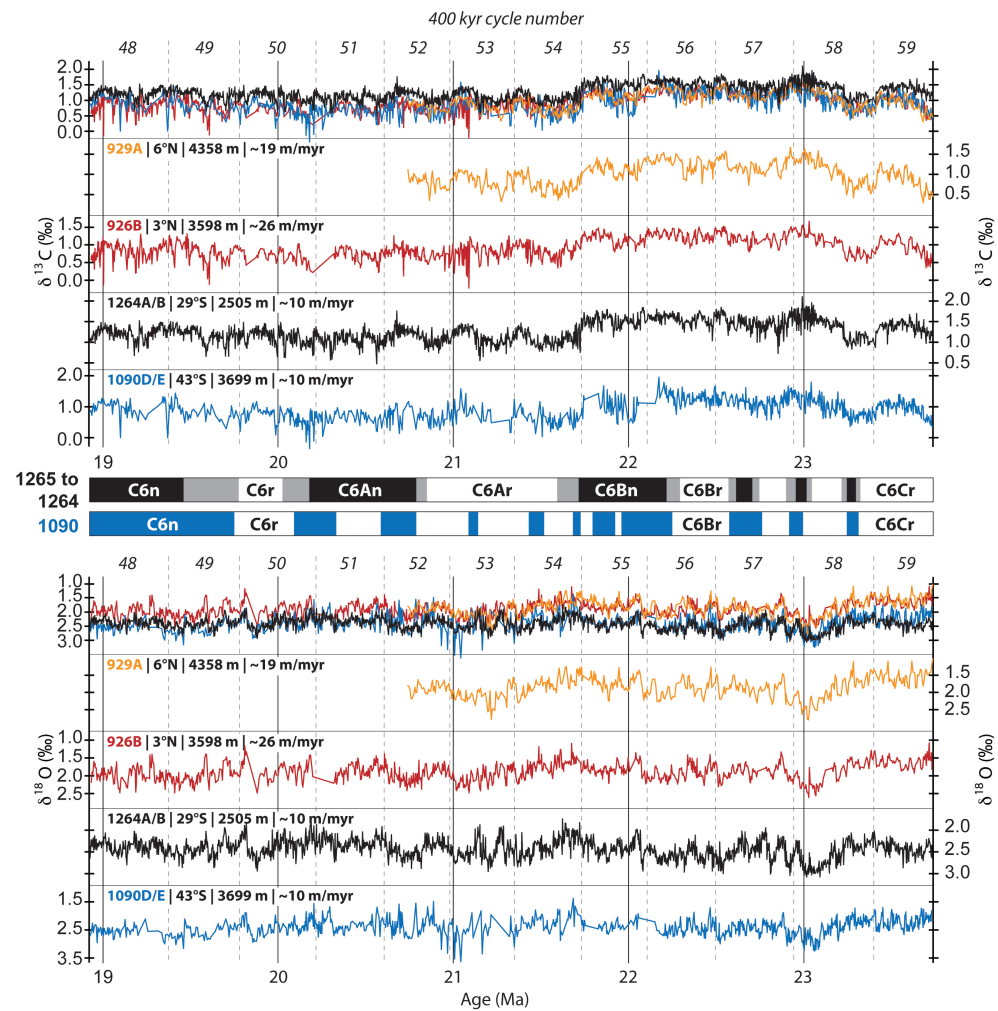
Back

Close

Full Screen / Esc

Printer-friendly Version

Interactive Discussion



**Dynamics of  
~100-kyr glacial  
cycles during the  
early Miocene**

D. Liebrand et al.

Title Page

Abstract

Introduction

Conclusions

References

Tables

Figures

◀

▶

◀

▶

Back

Close

Full Screen / Esc

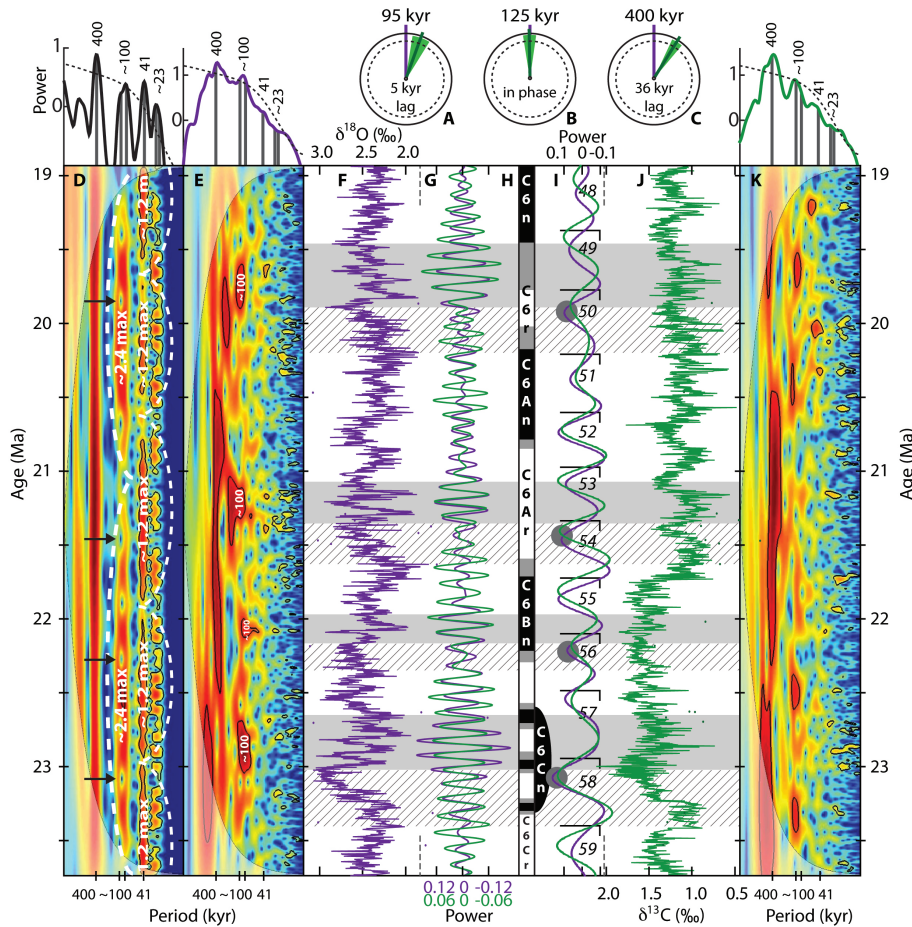
Printer-friendly Version

Interactive Discussion

**Fig. 3.** Comparison of early Miocene stable isotope records. High-resolution Atlantic  $\delta^{13}\text{C}$  and  $\delta^{18}\text{O}$  (+0.64‰) records of ODP Sites 926, 929, 1264 and 1090. Records were matched in the depth domain using the “Match” algorithm (Lisiecki and Lisiecki, 2002) and then plotted on the age model of Site 1264. The Walvis Ridge magnetostratigraphy (Bowles, 2006) has been transferred from Site 1265 to Site 1264 (see Fig. 2). The vertical dashed lines mark the boundaries of the 400-kyr cycles (Wade and Pälike, 2004). Latitude, present water depth and average sedimentation rates are given for each site.

**Dynamics of  
~100-kyr glacial  
cycles during the  
early Miocene**

D. Liebrand et al.



Discussion Paper | Discussion Paper | Discussion Paper | Discussion Paper | Discussion Paper

Title Page

Abstract

Introduction

Conclusions

References

Tables

Figures

◀

▶

◀

▶

Back

Close

Full Screen / Esc

Printer-friendly Version

Interactive Discussion



**Fig. 4.** Walvis Ridge stable isotope records. Phase wheels represent the phase relation between  $\delta^{13}\text{C}$  (green) and  $\delta^{18}\text{O}$  (purple) at the **(A)** 95, **(B)** 125 and **(C)** 400-kyr eccentricity periods, where  $360^\circ$  represents one full cycle. Phase lags increase clockwise and the green areas represent the 95% confidence level. Vector length shows coherency (dashed circle 95%). **(D)** Wavelet analysis (Grinsted et al., 2004) (the continuous wavelet transform expands the time series into time frequency space) with >95% confidence levels (black lines) of an eccentricity/obliquity/precession mix calculated after the astronomical solution (Laskar et al., 2004), with white dashed lines indicating the (on average)  $\sim 1.2$  and  $\sim 2.4$  myr amplitude modulation of obliquity and eccentricity. On top the global spectrum (Torrence and Compo, 1998) with >95% confidence level. **(E)** Wavelet analysis (Grinsted et al., 2004) with >95% confidence levels (black lines) of  $\delta^{18}\text{O}$  record after removal of >0.5 myr periodicities using a notch filter (Paillard et al., 1996) and normalization. On top the global spectrum (Torrence and Compo, 1998) with >95% confidence level. Arrows indicate minima in  $\sim 400$ -kyr eccentricity (characterised by a smaller amplitude  $\sim 100$ -kyr cycle) that coincide with maximum ice-sheet build-up. These minima lay 2 or  $4 \times 400$ -kyr apart. **(F)** Oxygen isotope ( $\delta^{18}\text{O} + 0.64\text{‰}$ ) record from Site 1264. Loose dots represent outliers. **(G)** Gaussian filters (Paillard et al., 1996) ( $\sim 100$ -kyr, f: 10.0, bw: 2.0) of the  $\delta^{18}\text{O}$  (purple) and  $\delta^{13}\text{C}$  (green) records. **(H)** Transferred magnetostratigraphy (Bowles, 2006) from Site 1265 to Site 1264. Black is normal, white is reversed, gray is uncertain. **(I)** Gaussian filters (Paillard et al., 1996) (400-kyr, f: 2.5, bw: 1.0) of the  $\delta^{18}\text{O}$  (purple) and  $\delta^{13}\text{C}$  (green) records, with corresponding 400-kyr cycle numbers (Wade and Pälike, 2004). Gray circles mark maximum of the ice-sheet build-up phases. **(J)** Carbon isotope ( $\delta^{13}\text{C}$ ) record from site 1264. Loose dots represent outliers. **(K)** Wavelet analysis (Grinsted et al., 2004) with >95% confidence levels (black lines) of  $\delta^{13}\text{C}$  record after removal of >0.5 myr periodicities using a notch filter (Paillard et al., 1996) and normalization. On top the global spectrum (Torrence and Compo, 1998) with >95% confidence level. Striped areas indicate periods with reduced  $\sim 100$ -kyr power, gray areas indicate  $\sim 100$ -kyr “worlds”.

## Dynamics of $\sim 100$ -kyr glacial cycles during the early Miocene

D. Liebrand et al.

Title Page

Abstract

Introduction

Conclusions

References

Tables

Figures

⏪

⏩

◀

▶

Back

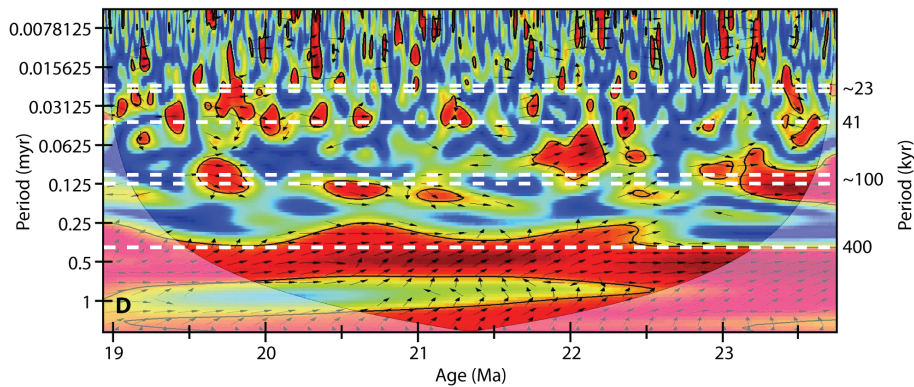
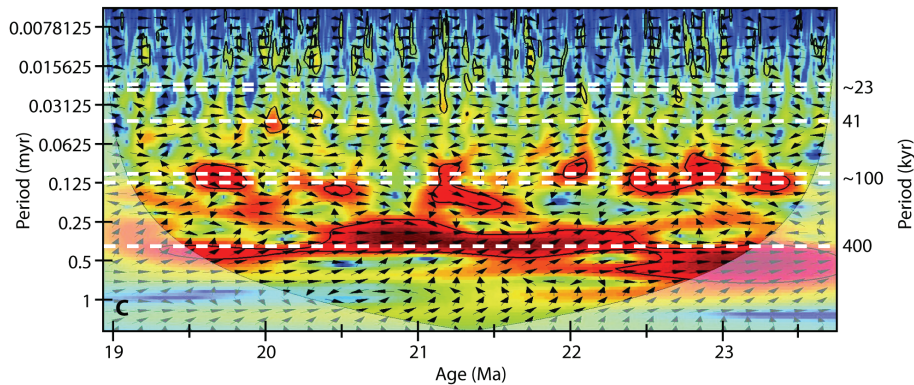
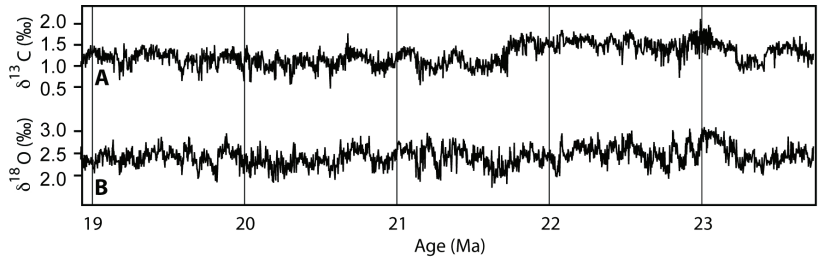
Close

Full Screen / Esc

Printer-friendly Version

Interactive Discussion





**Dynamics of  
 ~100-kyr glacial  
 cycles during the  
 early Miocene**

D. Liebrand et al.

Title Page

Abstract Introduction

Conclusions References

Tables Figures

◀ ▶

◀ ▶

Back Close

Full Screen / Esc

Printer-friendly Version

Interactive Discussion

## Dynamics of ~100-kyr glacial cycles during the early Miocene

D. Liebrand et al.

**Fig. 5.** Cross wavelet transform and wavelet coherence. **(A)**  $\delta^{13}\text{C}$  record from Site 1264 of the Walvis Ridge. **(B)**  $\delta^{18}\text{O}$  record from Site 1264 of the Walvis Ridge. **(C)** Cross wavelet transform analysis between the  $\delta^{18}\text{O}$  and  $\delta^{13}\text{C}$  records indicating regions in time frequency space where the time series show high common power (Grinsted et al., 2004). Phase arrows pointing right means  $\delta^{18}\text{O}$  and  $\delta^{13}\text{C}$  are in-phase. Phase arrows pointing left means  $\delta^{18}\text{O}$  and  $\delta^{13}\text{C}$  are in anti-phase. Phase arrows pointing down means that  $\delta^{18}\text{O}$  is leading  $\delta^{13}\text{C}$  by  $90^\circ$ . Phase arrows pointing up means that  $\delta^{13}\text{C}$  is leading  $\delta^{18}\text{O}$  by  $90^\circ$ . Black lines represent  $>95\%$  significance levels. **(D)** Wavelet coherence analysis (Grinsted et al., 2004) between the  $\delta^{18}\text{O}$  and  $\delta^{13}\text{C}$  records indicating regions in time frequency space where the two time series co-vary. However, they do not necessarily have high power on these frequencies (Grinsted et al., 2004). Phase arrows representation as in panel **(C)**. Black lines represent  $>95\%$  Monte Carlo significance levels. Regions in the time frequency space where both records show much power (panel **C**) and where both records are coherent (panel **D**) represent the coupling between climate states and the changes in the oceanic carbon reservoir which has also been described in other records (Zachos et al., 1997, 2001b; Paul et al., 2000).

Title Page

Abstract

Introduction

Conclusions

References

Tables

Figures

⏪

⏩

◀

▶

Back

Close

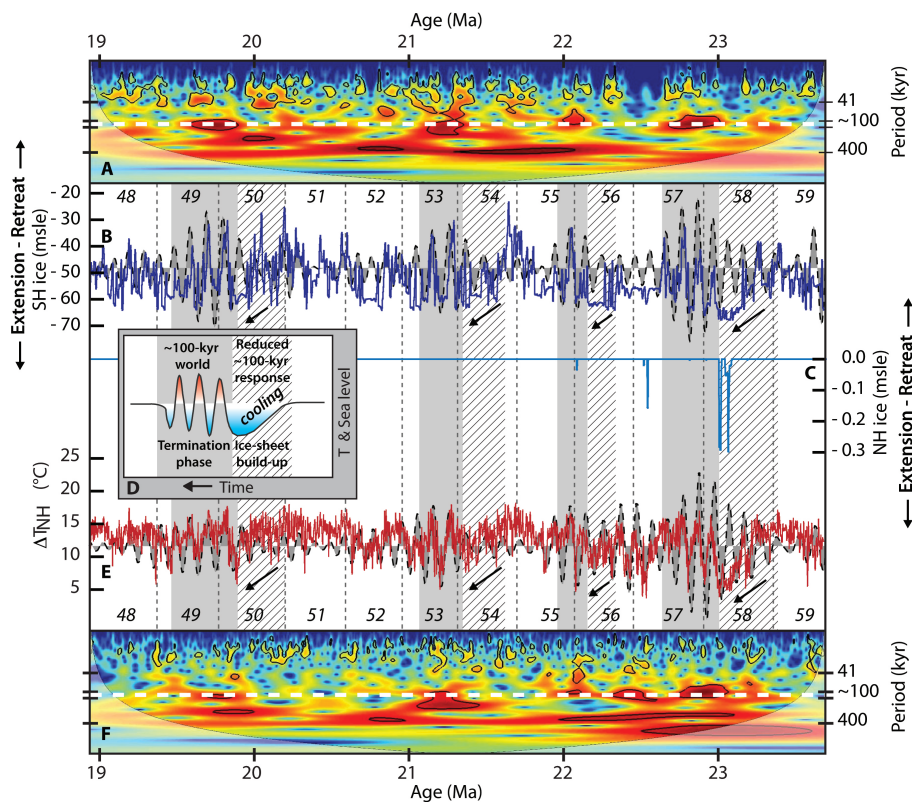
Full Screen / Esc

Printer-friendly Version

Interactive Discussion

## Dynamics of ~100-kyr glacial cycles during the early Miocene

D. Liebrand et al.



Title Page

Abstract

Introduction

Conclusions

References

Tables

Figures

◀

▶

◀

▶

Back

Close

Full Screen / Esc

Printer-friendly Version

Interactive Discussion

## Dynamics of ~100-kyr glacial cycles during the early Miocene

D. Liebrand et al.

**Fig. 6.** 1-D inverse modelling output (De Boer et al., 2010). **(A)** Wavelet analysis (Grinsted et al., 2004) (the continuous wavelet transform expands the time series into time frequency space) of Southern Hemisphere (Antarctic) ice variability (in meter sea level equivalent), after removal of  $>0.5$  myr periodicities using a notch filter (Paillard et al., 1996). White dotted line indicates the  $\sim 100$ -kyr period. **(B)** Antarctic ice, with  $\sim 100$ -kyr filtered component (f: 10.0, bw: 2.0) (Paillard et al., 1996) depicted in the background. **(C)** Northern Hemisphere (Greenland) ice volume. **(D)** Template depicting a generality in early Miocene climate. Climate deterioration (ice-sheet build-up phases, striped areas/downward pointing arrows) precedes  $\sim 100$ -kyr climate variability (termination phases, gray areas). The ice-sheet build-up phases (inception phase) are characterised by a less linear response to the  $\sim 100$ -kyr eccentricity cycle, while the termination phases show greater linear response. **(E)** Northern Hemisphere ( $40$ – $80^\circ$  latitude) annual average air temperature, with  $\sim 100$ -kyr filtered component (f:10.0, bw: 2.0) (Paillard et al., 1996) depicted in the background. **(F)** Wavelet analysis (Grinsted et al., 2004) of NH temperature variability. White dashed line indicates the  $\sim 100$ -kyr period. Vertical dashed lines and numbers in italic represent the 400-kyr cycle numbers (Wade and Pälike, 2004).

Title Page

Abstract

Introduction

Conclusions

References

Tables

Figures

⏪

⏩

◀

▶

Back

Close

Full Screen / Esc

Printer-friendly Version

Interactive Discussion



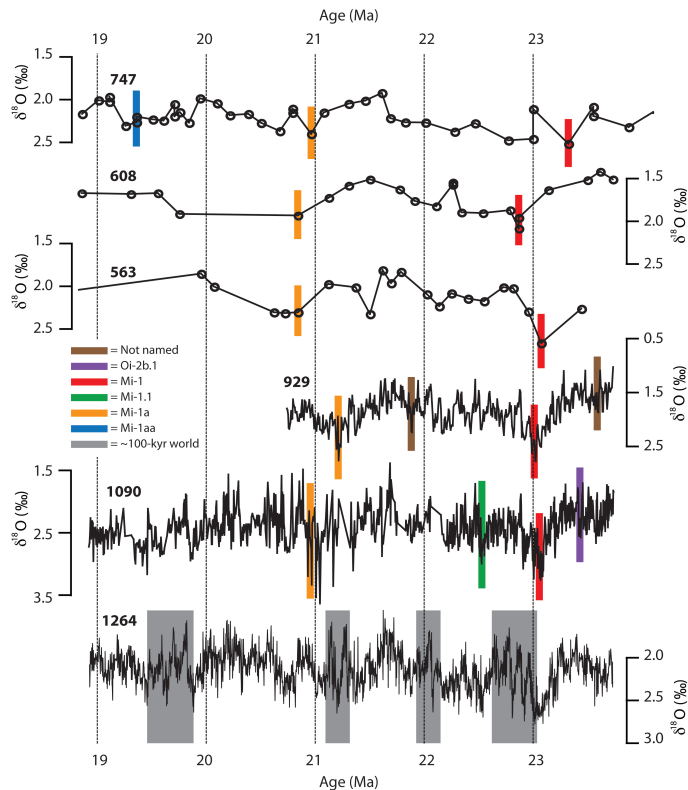


**Fig. 7.** Latest Oligocene and early Miocene Oi- and Mi-naming scheme. Comparison between isotope records from the Kuergellen Plateau site 747 and the North Atlantic Sites 563 and 608 (Wright et al., 1992; Wright and Miller, 1992) with Site 1264. Ages of Sites 563, 608 (Berggren et al., 1995) and magnetostratigraphy of site 747 (Oslick et al., 1994) have been recalculated to the ATNTS2004 (Lourens et al., 2004). Sites 929 and 1090 are plotted on the Walvis Ridge Site 1264 age model. The ~100-kyr “worlds” described in this study are close within the age estimates of the previously described Mi-1, Mi-1a and Mi-1aa zones or episodes.